

Microcalorimetric measurements of differential heats of adsorption on reactive catalyst surfaces

B. E. Spiewak, J. A. Dumesic *

Department of Chemical Engineering, University of Wisconsin-Madison, Madison, WI 53707, USA

Received 29 April 1996; accepted 26 June 1996

Abstract

Techniques are presented for measurement of differential heats of adsorption on reactive catalyst surfaces using heat-flux calorimetry. Samples are prepared *ex-situ* in ultra-pure flowing gases and then sealed in Pyrex capsules. Special calorimetric cells are employed to break the sample capsule after thermal equilibration of the sample with the calorimeter. In this manner the clean sample is exposed rapidly to the adsorbing gas, minimizing surface contamination. Initial heats of CO and H₂ adsorption at 403 K on Pt/SiO₂ catalysts obtained using the present technique (135 and 100 kJ/mol, respectively) were in agreement with results reported in the literature using standard calorimetric procedures. Initial heats measured in this study for CO adsorption at 308 K on reduced Ni powders (120 kJ/mol) and on nickel samples containing metallic potassium (200 kJ/mol) corresponded to values in the literature from ultrahigh vacuum studies of CO adsorption on Ni single crystal surfaces. The initial heat of N₂ adsorption at 453 K on reduced iron determined in this study (200 kJ/mol) was in agreement with results obtained in ultrahigh vacuum measurements of metallic iron single crystal surfaces. These results, for catalyst systems that are sensitive to traces of oxygen-containing species, provide strong evidence that the experimental techniques employed in the present study allow clean metallic surfaces to be maintained during microcalorimetric adsorption studies.

Keywords: Microcalorimetry; Platinum; Nickel; Iron; Alkali metals

1. Introduction

Heat-flow microcalorimetry can be used to provide direct measurements of heats of adsorption of molecules on solid surfaces over a wide range of temperatures (77–873 K), as illustrated in various reviews [1–9]. For example, microcalorimetry has been used to study acid sites in zeolites [10–26] and metal oxides [8,27–38], and also to probe sites on supported metal catalysts [39–62].

Typical microcalorimetric methods must be used carefully to study metal surfaces that may show high reactivity with impurities commonly encountered in high vacuum systems (e.g. O₂, H₂O, CO and CO₂). Furthermore, leak-rates into calorimetric cells may lead to excessive accumulation of contaminants on the surface during the times typically employed for thermal equilibration of the sample in the calorimeter (*ca.* 5–6 hours). In this paper, we describe a technique for using conventional heat-flux calorimetry to measure differential heats of adsorption on reactive metal surfaces. Briefly, a sample is

* Corresponding author.

prepared *ex-situ* with ultra-pure flowing gases, and sealed in a Pyrex capsule. This capsule is subsequently broken in the calorimetric cells after the capsule and cells have attained thermal equilibrium with the calorimeter. In this manner, the clean sample can be exposed rapidly to the adsorbate gases under study. The calorimetric results obtained with this method are compared to results obtained employing standard calorimetric methods and to ultrahigh vacuum results.

2. Experimental

2.1. Sample treatment

Ultrahigh purity (99.999%) H₂ and He (Liquid Carbonic) were used to treat all samples. These gases were purified by passage over heated (473 K) copper turnings to remove oxygen and activated molecular sieves (13X), cooled to 77 K, to remove water. The gases were further purified by passage over a bed of reduced Oxy-trap (Alltech Association, Inc) and a bed of reduced iron catalyst at room temperature to remove oxygenated impurities.

Samples were treated in a glass cell attached to a high-vacuum volumetric system (described below)

by means of a Pyrex 10/30 ground-glass joint. Pyrex vacuum stopcocks, greased with Apezion "N" (grease 1×10^{-7} Pa vapor pressure at 293 K), and thoroughly degassed at room temperature, were used to isolate the sample within the cell. A Pyrex NMR tube (Wilmad Glass, 5 mm in diameter and 18 cm long), sealed to the side of the treatment cell, served as both the fill port and a capsule in which to seal the sample.

2.2. System description

A schematic diagram of the microcalorimetric system is shown in Fig. 1. The microcalorimeter is a Setaram BT2.15D heat-flux calorimeter, capable of operation at temperatures from 77–473 K. A Setaram C80 heat-flux microcalorimeter (273–573 K) has also been used. The microcalorimeter is connected, by means of a specially designed set of calorimeter cells, to a volumetric system equipped with a vacuum system (dynamic vacuum of 10^{-5} Pa), a gas handling system with probe molecule reservoir, and a calibrated dosing volume employing MKS Baritron capacitance manometers for precision pressure measurement ($\pm 1 \times 10^{-2}$ Pa). The leak-rate of the volumetric system is 10^{-4} Pa/minute in a system volume of approximately 70 cm³ (i.e. 10^{-6} μmol/minute).

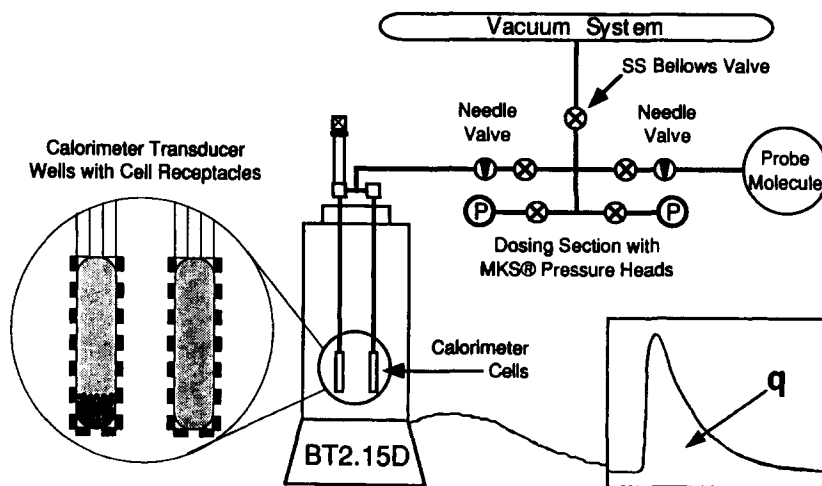


Fig. 1. Schematic diagram of the BT2.15D microcalorimetry apparatus.

2.3. Microcalorimetric cells

The microcalorimetric cells used to break the sealed Pyrex capsule, and subsequently, to allow adsorption measurements on the clean sample, are shown in Fig. 2. These cells are constructed of AISI type 316 stainless steel and measure about 85 cm long and about 10 cm wide. Two identical receptacles, one for the Pyrex sample capsule and the other for a reference capsule, are connected to the two ends of the cell stems with modified Cajon VCR fittings. The length (12.70 cm), diameter (1.67 cm),

and distance apart (6.67 cm) of these receptacles, were chosen to match the depth, diameter, and spacing of the transducer wells in the BT2.15D calorimeter, respectively (see Fig. 1). The Pyrex capsule containing the sample is placed in the sample receptacle, and an empty, openended Pyrex tube of equal length is placed in the reference receptacle to equate the heat transfer characteristics of the two receptacles. The cell stems are 0.40 cm outside diameter, thin wall (0.041 cm), stainless steel used to minimized conductive heat losses. A stainless steel baffle and three Teflon baffles are placed along each

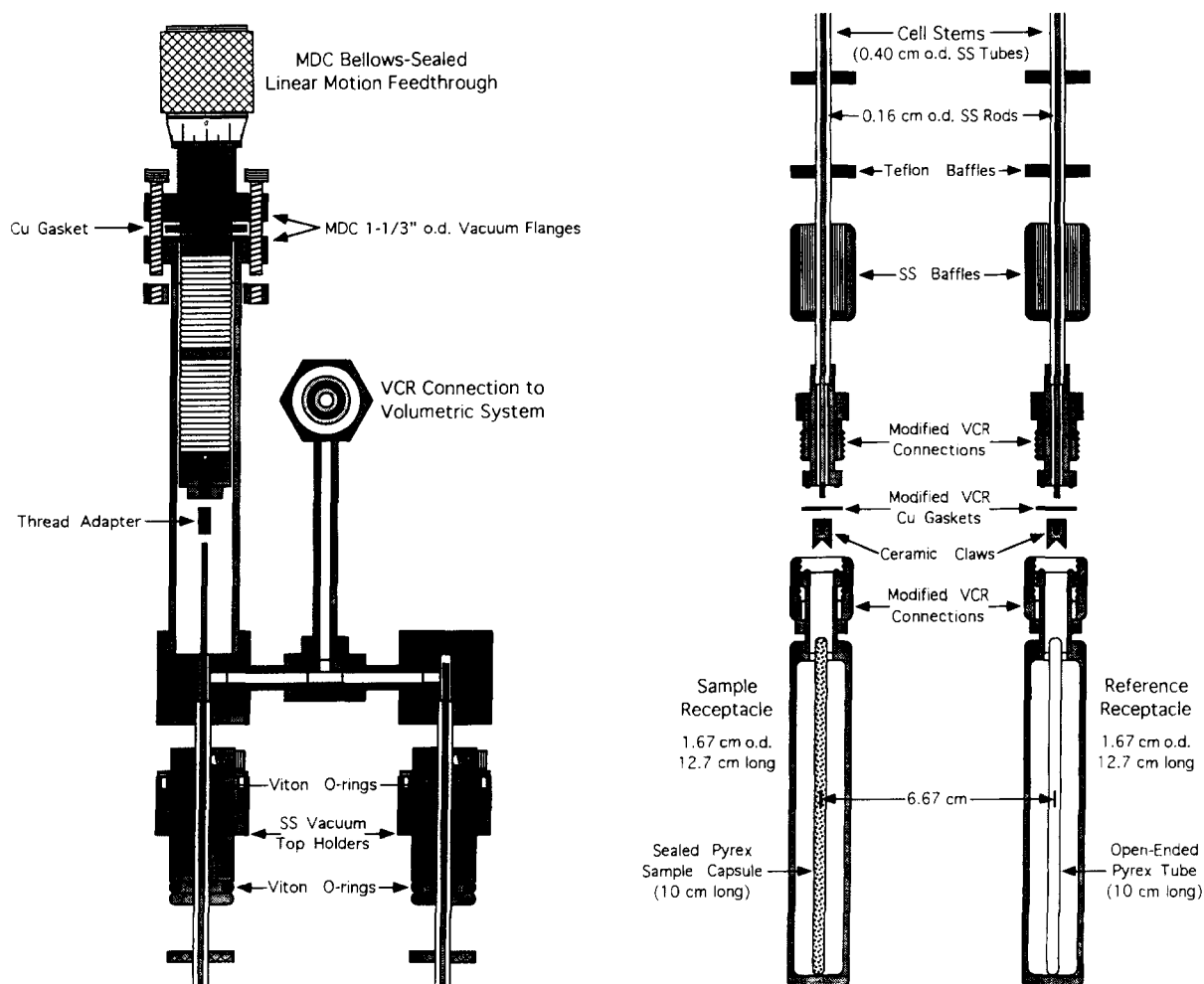


Fig. 2. Schematic diagram of the BT2.15D microcalorimeter cells.

of the cell stems to minimized convective air currents within the transducer wells. A stainless steel holder near the top of the cell stems, equipped with Viton O-rings, provides a seal between the cell stems and the transducer wells, and serves to isolate the cells in the calorimeter. The upper portion of the cells are fitted with a MDC bellows-sealed linear motion feedthrough, affixed to the top of the cells by means of standard, copper gasketed, 1–1/3 inch outside diameter vacuum flanges (MDC). The linear motion feed-through provides the driving force to break the sealed Pyrex capsule. A 0.16 cm outside diameter stainless steel rod, threaded into the end of the motion feedthrough and extending through the cell stem and into the sample receptacle, provides the length required to reach the sample capsule. A piece of machinable ceramic is threaded onto the other end of the stainless steel rod to form a sturdy surface for breaking the capsule. The ceramic also serves to eliminate conductive heat transfer out the top of the sample receptacle. A similar stainless steel rod and ceramic assembly, threaded directly into the calorimetric cells, is placed on the reference side to further equate the heat transfer characteristics of the sample and reference receptacles. The cells are connected to the volumetric system by means of standard Cajon VCR fittings.

2.4. Procedures

In a typical experiment, a measured mass of sample (typically 0.5–5 g) is loaded into the glass cell, followed by treatment in flowing gases, e.g., calcination in flowing oxygen and reduction to the metallic state in flowing hydrogen at elevated temperatures (e.g., 723 K). Upon completion of the treatment cycle, the sample is purged with helium (ca. 2 hours) at elevated temperature to remove adsorbed gases, cooled to room temperature in flowing helium, and subsequently evacuated to ca. 5×10^4 Pa of helium. The sample is then transferred into the attached Pyrex NMR tube and sealed with a torch in a 10 cm long section of the tube. The sample capsule formed in this manner is loaded into the sample receptacle of the calorimetric cells, which are subsequently immersed in the isothermal calorimetric block. The cells are evacuated to ca. 10^{-4} Pa and allowed to reach thermal equilibrium

with the calorimeter (ca. 5–6 hours), at which point a stable differential heat response (baseline) is achieved.

The microcalorimetric measurements are initiated by breaking the Pyrex sample capsule within the calorimetric cells. The helium obtained upon breaking the capsule is evacuated to ca. 0.1 kPa, which serves as a heat transfer medium between the sample and the walls of the calorimeter cell. Once the differential heat response stabilizes (ca. 15–30 minutes), doses of the adsorbate (1–10 μmol quantities) are sequentially admitted to the sample until it becomes saturated. The resulting heat response for each dose is recorded as a function of time and subsequently integrated to determine the amount of the heat generated (mJ). The amount of gas adsorbed ($\mu\text{mol/g}$) is determined volumetrically from the dose and equilibrium pressures, and the system volumes and temperatures. The differential heat (kJ/mol), defined as the negative of the enthalpy change of adsorption per mole of gas adsorbed, is then calculated for each dose by dividing the heat generated by the amount of gas adsorbed.

3. Results/Discussion

3.1. Calibration experiments

It is necessary to compare the results obtained using the above procedures with data collected with more traditional microcalorimetric methods for a catalyst sample that is not particularly sensitive to the trace components typically found in high vacuum systems. Such a system is supported platinum, since this metal is easily reduced to the zero-valent state at room temperature [63]. Accordingly, heats of H_2 and CO adsorption at 403 K were measured on metal catalysts consisting of 0.85 and 1.2 wt% platinum supported on silica. Figure 3 shows the results for H_2 adsorption at 403 K on the 1.2 wt% Pt/ SiO_2 catalyst and Fig. 4 shows the results for CO adsorption at 403 K on the 0.85 wt% Pt/ SiO_2 catalyst, collected according to standard calorimetric procedures employed in previous studies [49,51] and compared to the results obtained using the present calorimetric technique. Initial heats of 90–100 kJ/mol were obtained for H_2 adsorption on the

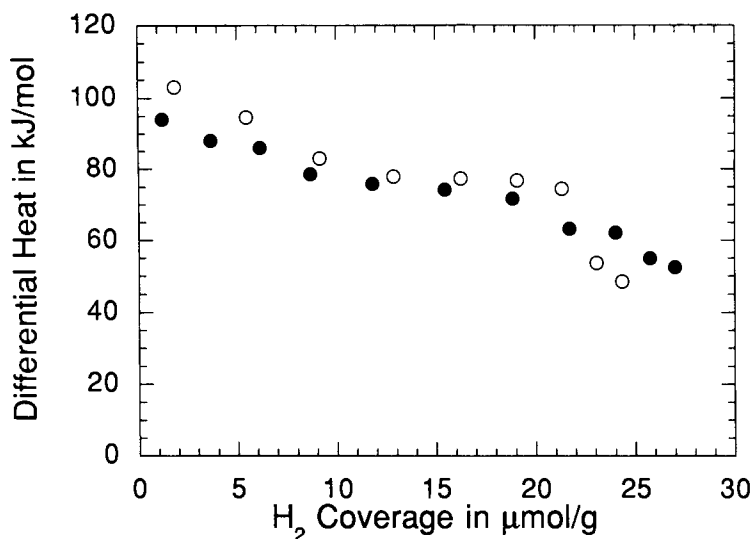


Fig. 3. Differential heat of H_2 adsorption at 403 K on 1.2 wt% Pt/SiO₂ employing standard calorimetric procedures (●) and the calorimetric technique presented here (○).

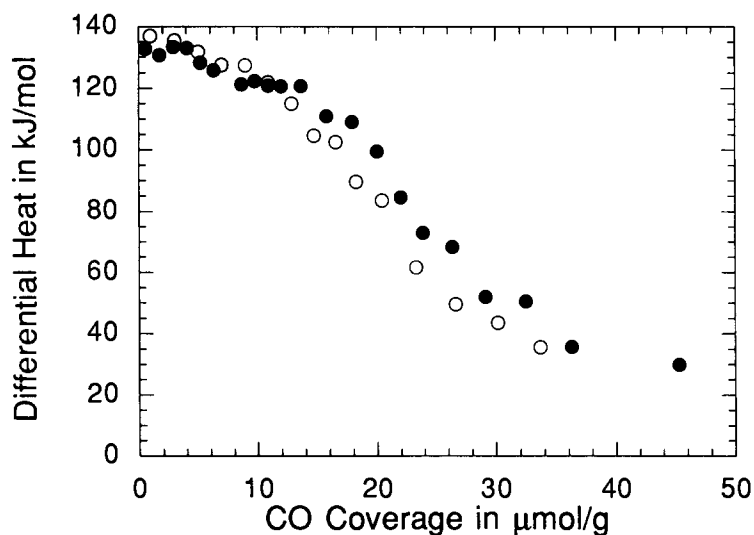


Fig. 4. Differential heat of CO adsorption at 403 K on 0.85 wt% Pt/SiO₂ employing standard calorimetric procedures (●) and the calorimetric technique presented here (○).

1.2 wt% Pt/SiO₂ catalyst, using both calorimetric methods, in excellent agreement with the heats of 93 [51], 91 ± 5 , and 92 ± 5 kJ/mol [49] reported for H_2 adsorption at 403 K on Pt/SiO₂ catalysts containing 1.2, 4.0 and 7.0 wt% platinum, respectively.

Similarly, initial heats of 140 kJ/mol were obtained for CO adsorption on the 0.85 wt% Pt/SiO₂ catalyst, using both calorimetric methods, in excellent agreement with the heats of 140 kJ/mol [49,51] reported for CO adsorption at 403 K on Pt/SiO₂

catalyst containing 1.2, 4.0 and 7.0 wt% platinum. Moreover, the differential heats decrease with adsorbate coverage for both calorimetric methods, until saturation coverages of 25 and 35 $\mu\text{mol/g}$ are reached for H_2 and CO, respectively. Thus, the calorimetric technique presented here gives results equivalent to those obtained using standard calorimetric methods for samples that are not particularly sensitive to the trace components typically present in high vacuum systems.

Nickel is a less-noble Group VIII metal compared to platinum, and it is informative to compare results obtained using the technique presented here for a low-surface area nickel powder with data collected under ultra-high vacuum conditions for nickel single-crystal surfaces. In this respect, nickel remains in the zero-valent state at room temperature for $\text{H}_2\text{O}/\text{H}_2$ ratios up to ca. 10^3 [64]. Figure 5 shows microcalorimetric results collected according to the procedures outlined in the present paper for CO adsorption at 308 K on a reduced nickel powder [65], as well as microcalorimetric data obtained under ultra-high vacuum conditions by King and co-workers [66] for CO adsorption at 300 K on Ni(100). The saturation coverage of CO on the nickel powder (22 $\mu\text{mol/g}$) has been normalized to

unity to facilitate comparison with the results for the Ni(100) surface. An initial heat of 120 kJ/mol was measured for CO adsorption on nickel powder, in good agreement with the value 123 ± 2 kJ/mol reported for Ni(100) [67]. These results show that a clean, metallic nickel surface can be prepared and maintained using the present calorimetric technique.

3.2. Nickel powders promoted with potassium and cesium

Nickel catalysts often contain alkali metal additives that may neutralize the support acidity, catalyze coke removal, and desensitize the catalysts toward poisoning [68]. The present microcalorimetric technique has been used to study effects of potassium and cesium addition to reduced nickel powders. These alkali metals are very reactive with oxygenated species such as dioxygen and water, and studies of these systems should, therefore, provide a sensitive test of surface cleanliness. In particular, potassium and cesium remain in the zero-valent state at room temperature in an atmosphere of H_2 for H_2O pressures lower than 10^{-22} and 10^{-20} Pa, respectively [64]. Microcalorimetric results for CO adsorption at 308 K on reduced nickel powders

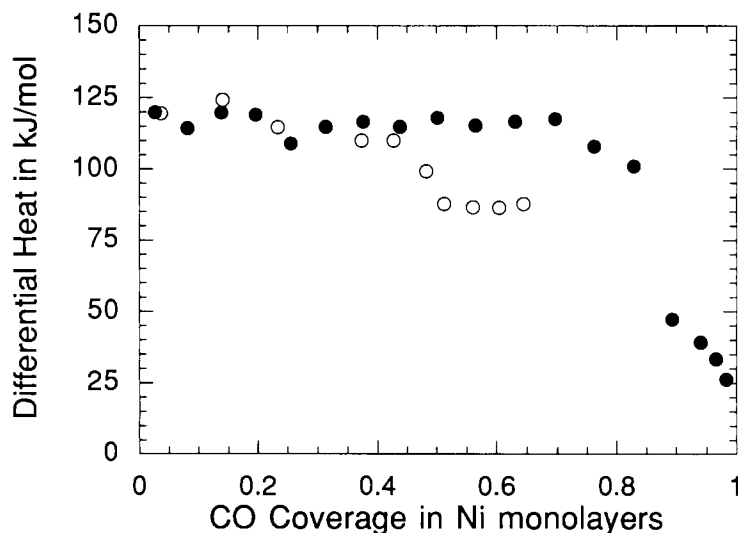


Fig. 5. Differential heat of CO adsorption at 308 K on nickel powder (●) [65]. Also shown are results for CO adsorption at 300 K on Ni(100) [66] (○). The CO coverage has been normalized with respect to the saturation coverage (22 $\mu\text{mol/g}$) for comparison with the single crystal results.

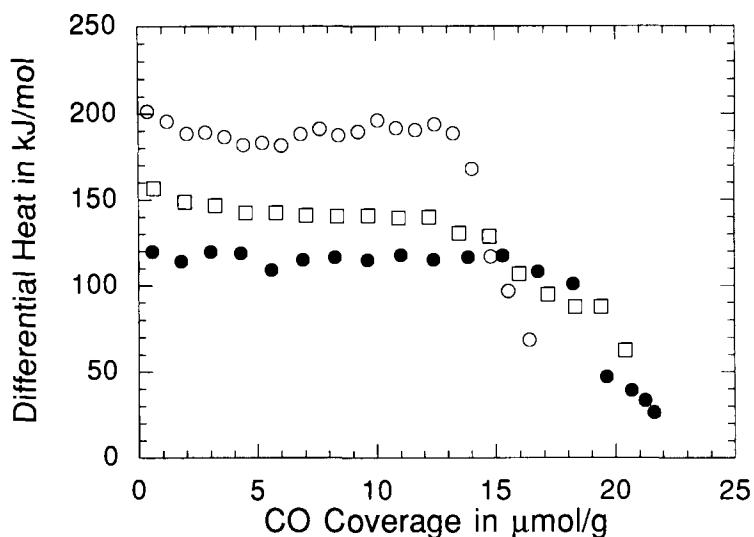


Fig. 6. Differential heat of CO adsorption at 308 K on nickel powder (●), potassium-promoted nickel ($\theta_K = 0.09\text{--}0.11$) (○), and the previous sample after exposure to air and subsequent reduction in H_2 at 623 K ($\theta_K = 0.21$) (□). Potassium coverages were measured by AES.

containing submonolayer amounts of potassium are shown in Fig. 6 [65]. The addition of 9–11% monolayer coverage of metallic potassium increases the initial heat of CO adsorption from 120 kJ/mol for the clean nickel surface to 200 kJ/mol. This high initial heat of CO adsorption is in agreement with the initial heat of 190 kJ/mol reported by King et al. [69] for CO adsorption on Ni(100) containing 8% monolayer coverage of metallic potassium. Exposure of the metallic potassium-promoted nickel powder to air, followed by reduction in H_2 at 623 K, results in a decrease in the initial heat of CO adsorption from 200 to 160 kJ/mol, indicating that the potassium on this sample is probably in a partially oxidized state, having a weaker promotional effect on CO adsorption.

The addition of submonolayer amounts of cesium to reduced nickel powders produced similar results [65]. The addition of 60% monolayer coverage of metallic cesium increases the initial heat of CO adsorption from 120 to 205 kJ/mol, and the differential heat remains nearly constant at ca. 185 kJ/mol to a CO coverage of 13 $\mu\text{mol/g}$. Oxidation of this sample and subsequent reduction in H_2 at 623 K, decreases the initial heat of CO adsorption to 160 kJ/mol and lowers the average differential heat to ca. 145 kJ/mol.

These results show that the presence of metallic potassium or cesium promote the adsorption of CO on nickel by increasing the strength of CO adsorption, in agreement with ultrahigh vacuum microcalorimetric measurements of CO adsorption on Ni(100) containing metallic potassium [66,69–72]. Exposure of these metallic alkali-containing samples to air and subsequent reduction in hydrogen, weakens the promotional effects observed for CO adsorption (i.e. the initial heats of CO adsorption are reduced by 40 kJ/mol), suggesting that it is difficult to prepare nickel surfaces containing metallic potassium or cesium by starting with alkali salts followed by reduction in H_2 at 623 K. These results provide strong evidence that the experimental techniques employed in our study allow reduced alkali metal additives on nickel to be maintained in the zero-valent state during microcalorimetric studies of CO adsorption.

3.3. Platinum catalysts promoted with alkali metals

Supported platinum catalysts find numerous applications in hydrocarbon conversion reactions [73]. For example, silica-supported Pt/Sn catalysts can be used for the selective dehydrogenation of

isobutane to isobutylene, an olefin used in the production of oxygenated compounds (e.g. MTBE, ETBE, TBA) required in reformulated gasoline [51]. The addition of potassium salts to these silica-supported Pt/Sn catalysts, followed by treatment in H_2 at 723 K, increases the rate of isobutane dehydrogenation, enhances dehydrogenation selectivity, and decreases the rate of catalyst deactivation [52].

The present microcalorimetric technique has been used to study the effect of alkali metal promoters on reduced platinum powders and silica-supported Pt and Pt/Sn isobutane dehydrogenation catalysts [74]. Figure 7 shows the microcalorimetric results for CO adsorption at 403 K on reduced platinum powders containing metallic rubidium and cesium. The addition of 40% monolayer coverage of metallic rubidium increases the initial heat of CO adsorption from 140 kJ/mol for the clean platinum surface to 160 kJ/mol. The differential heat remains constant at this value for the first 20 $\mu\text{mol/g}$ of CO coverage, and then decreases to 110 kJ/mol, where it remains until the sample becomes saturated with CO at a coverage of ca. 120 $\mu\text{mol/g}$. Similarly, the addition of 80% monolayer coverage of metallic cesium to platinum powder increases the initial heat of CO adsorption from 140 to 180 kJ/mol. As with

metallic rubidium, the differential heat remains constant at 180 kJ/mol to a CO coverage of ca. 18 $\mu\text{mol/g}$, and it then decreases to 115 kJ/mol and remains constant until a saturation CO coverage of ca. 60 $\mu\text{mol/g}$. These results show that metallic rubidium and cesium promote the adsorption of CO on platinum by strengthening the Pt–CO bond and by extending the CO adsorption capacity. The increase in adsorption capacity can be attributed to the formation of an alkali–CO complex on platinum at 403 K [74].

The differential heats of CO adsorption at 403 K on silica-supported Pt/Sn isobutane dehydrogenation catalysts containing alkali promoters, deposited from alkali salts followed by treatment in H_2 at 723 K, were similar to the behavior of the corresponding unpromoted catalysts [74]. For example, the presence of sodium and cesium (1:3 atomic Pt:alkali ratio) on a 2:1 Pt/Sn/SiO₂ catalyst (2.61 wt% platinum), had no effect on the initial heat of CO adsorption; however, these additives resulted in a significant reduction in the CO saturation uptakes.

These results show that the alkali promoters are not in the metallic state on these silica-supported Pt/Sn isobutane dehydrogenation catalysts. The re-

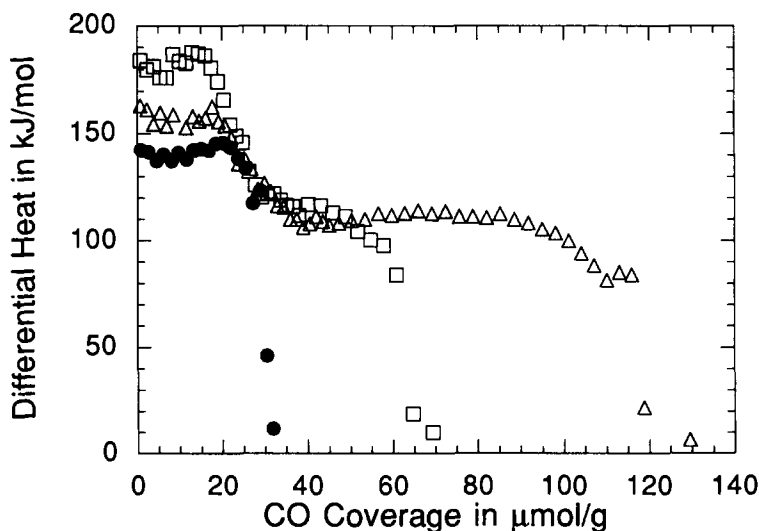


Fig. 7. Differential heat of CO adsorption at 403 K on platinum powder (●), rubidium-promoted platinum ($\theta_{Rb} = 0.4$) (Δ), and cesium-promoted platinum ($\theta_{Cs} = 0.8$) (□). Alkali coverages were measured by AES.

duction in the CO saturation coverage observed for the alkali-promoted Pt/Sn/SiO₂ samples, suggests that tin may anchor the alkali to the platinum surface, blocking CO adsorption sites, which may in part account for the observed promotional effects of potassium on Pt/Sn/SiO₂ [52].

3.4. Reduced iron

Ammonia is produced from the reaction between hydrogen and nitrogen over a reduced iron catalyst, typically at 823 K and 10 Mpa. The rate-determining step in the reaction is the dissociation of the diatomic nitrogen molecule [75]. Alumina is typically added (1–10% wt% Al) to iron catalysts to increase the available iron surface area, and subsequently, increase catalyst activity. The addition of potassium (1–3 wt% K) to these iron catalysts increases catalytic activity per unit surface area [76–78].

The present microcalorimetric technique has been used to measure differential heats of N₂ adsorption on reduced iron, to probe the iron-nitrogen interaction and the effect of promoters [79]. It is worthy to note that N₂ adsorption sites on metallic iron surfaces have been shown to be blocked by traces of oxygen-containing species [80], making this system a sensitive test of the effectiveness of the experimental procedures outlined in this paper. Moreover, iron remains in the zero-valent state at room temperature for H₂O/H₂ ratios less than 10⁻⁴ [64]. Figure 8 shows the results for N₂ adsorption at 453 K on a reduced singly-promoted (Al₂O₃) iron sample, provided by Haldor Topsøe, Inc. The initial heat of N₂ adsorption is ca. 200 kJ/mol, and the differential heat declines gradually with increasing N₂ coverage until the surface becomes saturated at a coverage of ca. 10 μmol/g.

For the purpose of the present study, the most important results from these studies of N₂ adsorp-

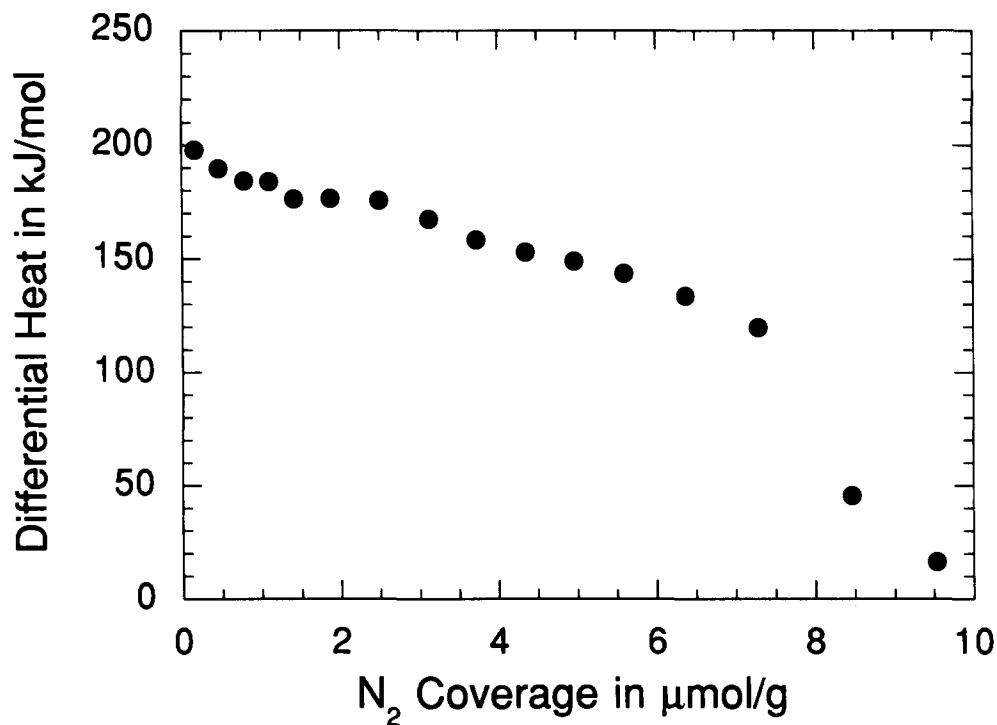


Fig. 8. Differential heat of N₂ adsorption at 453 K on singly-promoted (Al₂O₃) iron sample.

tion on reduced iron is that the initial heat of N₂ adsorption, near 200 kJ/mol, is in excellent agreement with estimates of the heats of N₂ dissociative adsorption (205–222 kJ/mol) on clean iron single crystal surfaces [81–83]. This good agreement again provides strong evidence that the experimental techniques employed in our study allow clean metallic surfaces to be maintained during microcalorimetric adsorption studies.

4. Conclusions

Techniques were developed for measuring differential heats of adsorption on reactive catalyst surfaces, using conventional heat-flux calorimetry. The method involves preparing a sample *ex-situ* in ultra-pure flowing gases, and then sealing the sample in a capsule of Pyrex. Microcalorimetric cells, employing a bellows-sealed linear motion feedthrough, provide the means to break the sample capsule after the sample and calorimetric cells have equilibrated thermally in the calorimeter. In this manner the clean sample is exposed rapidly to the adsorbing gas, minimizing surface contamination by impurities typically found in high vacuum systems.

Differential heats of CO and H₂ adsorption at 403 K on silica-supported Pt catalysts, obtained using the present technique, were shown to be identical to the results obtained using standard calorimetric procedures. Thus, the calorimetric technique presented here gives results equivalent to those obtained using standard calorimetric methods for samples that are not particularly sensitive to contamination by components typically present in high vacuum systems. Differential heats of CO adsorption at 308 K on reduced nickel powder and on nickel surfaces containing sub-monolayer amounts of metallic potassium were shown to be equal to results obtained from ultrahigh vacuum microcalorimetric measurements of CO adsorption at 300 K on nickel single crystal surfaces. In addition, results of studies of N₂ adsorption on reduced iron were shown to be in agreement with results obtained in ultrahigh vacuum measurements. These results, for catalyst systems that are very sensitive to traces of oxygen-containing species, provide strong evidence that the experimental techniques employed

in our study allow clean metallic surfaces to be maintained during microcalorimetric adsorption studies.

Acknowledgments

This work was supported by a research grant from the National Science Foundation. We are grateful to Bill Cotter at the UW Physical Sciences Laboratory for construction of the microcalorimetric cells. We also thank Birgit Fastrup at Haldor Topsøe, Inc. for providing to us the iron-based samples, and Dr. Jianyi Shen, Erik Haralson, and Manuel Natal-Santiago for their help with the calorimetric experiments.

References

- [1] P. C. Gravelle, *Adv. Catal.*, 22 (1972) 191.
- [2] P. C. Gravelle, in J. W. Hightower (ed.), *Proceedings of the Fifth International Congress on Catalysis*, Vol. 1, North-Holland Publishing, Amsterdam, 1973, p. 65.
- [3] P. C. Gravelle, *Catal. Rev.-Sci. Eng.*, 16 (1977) 37.
- [4] P. C. Gravelle, *Thermochim. Acta*, 96 (1985) 365.
- [5] V. E. Ostrovsky, *J. Therm. Anal.*, 14 (1978) 27.
- [6] G. Wedler, *J. Therm. Anal.*, 14 (1978) 15.
- [7] G. Della Gatta, *Thermochim. Acta*, 96 (1985) 349.
- [8] N. Cardona-Martinez and J. A. Dumesic, *Adv. Catal.*, 38 (1992) 149.
- [9] B. E. Spiewak, R. D. Cortright and J. A. Dumesic, in G. Ertl, H. Knözinger and J. Weitkamp (ed.), *Handbook of Heterogeneous Catalysis*, Vol. A, in press, 1996.
- [10] D. T. Chen, S. B. Sharma, I. Filimonov and J. A. Dumesic, *Catal. Lett.*, 12 (1992) 201.
- [11] D. Chen, et al., *J. Catal.*, 136 (1992) 392.
- [12] D. T. Chen, L. Zhang, C. Yi and J. A. Dumesic, *J. Catal.*, 146 (1994) 257.
- [13] B. E. Spiewak, B. E. Handy, S. B. Sharma and J. A. Dumesic, *Catal. Lett.*, 23 (1994) 207.
- [14] D. J. Parrillo and R. J. Gorte, *Catal. Lett.*, 16 (1992) 17.
- [15] D. J. Parrillo, R. J. Gorte and W. E. Farneth, *J. Am. Chem. Soc.*, 115 (1993) 12441.
- [16] D. J. Parrillo and R. J. Gorte, *J. Phys. Chem.*, 97 (1993) 8786.
- [17] R. J. Gorte and W. E. Farneth, to be published (1995).
- [18] H. Karge and V. Dondur, *J. Phys. Chem.*, 94 (1990) 765.
- [19] A. Auroux, et al., *J. Chem. Soc. Faraday Trans.*, 1, 75 (1979) 2544.
- [20] A. Auroux, P. Wierzchowski and P. C. Gravelle, *Thermochim. Acta*, 32 (1979) 165.
- [21] J. C. Vedrine, et al., *J. Catal.*, 59 (1979) 248.
- [22] A. Auroux, M. B. Sayed and J. C. Vedrine, *Thermochim. Acta*, 93 (1985) 557.
- [23] A. Auroux and Y. B. Taarit, *Thermochim. Acta*, 122 (1987) 63.

- [24] A. Auroux, Y. S. Jin, J. C. Vedrine and L. Benoist, *Appl. Catal.*, 36 (1988) 323.
- [25] A. Macedo, et al., *ACS Symp. Ser.*, 368 (1988) 98.
- [26] Z. C. Shi, A. Auroux and Y. B. Taarit, *Can. J. Chem.*, 66 (1988) 1013.
- [27] N. Cardona-Martinez and J. A. Dumesic, *J. Catal.*, 125 (1990) 427.
- [28] N. Cardona-Martinez and J. A. Dumesic, *J. Catal.*, 127 (1991) 706.
- [29] N. Cardona-Martinez and J. A. Dumesic, *J. Catal.*, 128 (1991) 23.
- [30] J. Shen, R. D. Cortright, Y. Chen and J. A. Dumesic, *Catal. Lett.*, 26 (1994)
- [31] J. Shen, R. D. Cortright, Y. Chen and J. A. Dumesic, *J. Phys. Chem.*, 98 (1994) 8067.
- [32] K. B. Fogash, et al., *Catal. Lett.*, 32 (1995) 241.
- [33] A. Auroux and A. Gervasini, *J. Phys. Chem.*, 94 (1990) 6371.
- [34] A. Gervasini and A. Auroux, *J. Therm. Anal.*, 37 (1991) 1737.
- [35] G. C. Colorio, A. Auroux and Bonnetot, *J. Therm. Anal.*, 38 (1992) 2565.
- [36] G. C. Colorio, A. Auroux and B. Bonnetot, *J. Therm. Anal.*, 40 (1993) 1267.
- [37] J. Le Bars, et al., *J. Phys. Chem.*, 96 (1992) 2217.
- [38] J. Le Bars and A. Auroux, *J. Therm. Anal.*, 40 (1993) 1277.
- [39] M. A. Vannice, L. C. Hasselbring, and B. Sen, *J. Catal.*, 95 (1985) 57.
- [40] M. A. Vannice, L. C. Hasselbring and B. Sen, *J. Catal.*, 97 (1986) 66.
- [41] B. Sen, P. Chou and M. A. Vannice, *J. Catal.*, 101 (1986) 517.
- [42] B. Sen and M. A. Vannice, *J. Catal.*, 130 (1991) 9.
- [43] A. Vannice and P. Chou, *J. Chem. Soc., Chem. Commun.*, 23 (1984) 1590.
- [44] M. A. Vannice and P. Chou, *ACS Symp. Ser.*, 298 (1986) 76.
- [45] P. Chou and M. A. Vannice, *J. Catal.*, 104 (1987) 1.
- [46] P. Chou and M. A. Vannice, *J. Catal.*, 104 (1987) 17.
- [47] P. Chou and M. A. Vannice, *J. Catal.*, 105 (1987) 342.
- [48] K. L. Anderson, J. K. Plischke and M. A. Vannice, *J. Catal.*, 128 (1991) 148.
- [49] S. B. Sharma, J. T. Miller and J. A. Dumesic, *J. Catal.*, 148 (1994) 198.
- [50] S. B. Sharma, et al., *J. Catal.*, 150 (1994) 234.
- [51] R. D. Cortright and J. A. Dumesic, *J. Catal.*, 148 (1994) 771.
- [52] R. D. Cortright and J. A. Dumesic, *J. Catal.*, 157 (1995) 1.
- [53] A. S. Gow and J. Phillips, *Energy Fuels*, 7 (1993) 674.
- [54] A. S. Gow III and J. Phillips, *Energy Fuels*, 6 (1992) 526.
- [55] M. O'Neil, R. Lovrien and J. Phillips, *Rev. Sci. Instrum.*, 56 (1985) 2312.
- [56] M. O'Neil and J. Phillips, *J. Phys. Chem.*, 91 (1987) 2867.
- [57] R. W. Wunder, et al., *Langmuir*, 9 (1993) 984.
- [58] J. Cobes and J. Phillips, *J. Phys. Chem.*, 95 (1991) 8776.
- [59] R. R. Gatte and J. Phillips, *Langmuir*, 5 (1989) 768.
- [60] J. Phillips and R. R. Gatte, *Thermochim. Acta*, 154 (1989) 13.
- [61] R. R. Gatte and J. Phillips, *J. Catal.*, 116 (1989) 49.
- [62] R. R. Gatte and J. Phillips, *Thermochim. Acta*, 133 (1988) 149.
- [63] J. E. Benson and M. Boudart, *J. Catal.*, 4 (1965) 704.
- [64] J. A. Dean (ed.), *Lange's Handbook of Chemistry*, 14th Edition, McGraw-Hill, Inc., New York, 1992.
- [65] B. E. Spiewak, J. Shen and J. A. Dumesic, *J. Phys. Chem.*, 99 (1995) 17640.
- [66] N. Al-Sarraf, J. T. Stuckless, C. E. Wartnaby and D. A. King, *Surf. Sci.*, 283 (1993) 427.
- [67] N. Al-Sarraf and D. A. King, *Surf. Sci.*, 307–309 (1994) 1.
- [68] D. W. Goodman, in H. P. Bonzel, A. M. Bradshaw and G. Ertl (ed.), *Physics and Chemistry of Alkali Metal Adsorption*. Elsevier, Amsterdam, 1989, p. 293.
- [69] N. Al-Sarraf, J. T. Stuckless and D. A. King, *Nature*, 360 (1992) 243.
- [70] M. P. Kiskinova, *Surf. Sci.*, 111 (1981) 584.
- [71] J. Lee, et al., *J. Chem. Phys.*, 82 (1985) 485.
- [72] L. J. Whitman and W. Ho, *J. Chem. Phys.*, 83 (1985) 4808.
- [73] C. N. Satterfield, *Heterogeneous Catalysis in Industrial Practice*, 2nd Edition, McGraw-Hill, Inc., New York, 1991, 554 pages.
- [74] B. E. Spiewak and J. A. Dumesic, *J. Phys. Chem.* (1996), in press.
- [75] P. H. Emmett, in E. Drauglis and R. I. Jaffee (ed.), *The Physical Basis for Heterogeneous Catalysis*, Plenum, New York, 1975, p. 3.
- [76] A. Nielsen, *Cat. Rev.*, 4 (1970) 1.
- [77] G. Ertl, *Cat. Rev.-Sci. Eng.*, 21 (1980) 201.
- [78] L. M. Aparicio and J. A. Dumesic, *Topics in Catalysis*, 1 (1994) 233.
- [79] B. E. Spiewak and J. A. Dumesic, to be published (1996).
- [80] B. Fastrup and H. N. Nielsen, *Catal. Lett.*, 14 (1992) 233.
- [81] G. Ertl, M. Grunze and M. Weiss, *J. Vac. Sci. Technol.*, 13 (1976) 314.
- [82] F. Bozso, G. Ertl, M. Grunze and M. Weiss, *J. Catal.*, 49 (1977) 18.
- [83] F. Bozso, G. Ertl and M. Weiss, *J. Catal.*, 50 (1977) 519.